Aerodynamics of an Ultralight Load-Aligned Rotor for Extreme-Scale Wind Turbines

Adam Steele[1], Brian Ichter[2], Chao Qin[3], Eric Loth[4]
University of Virginia, Charlottesville, VA, 22904

Michael Selig[5]
University of Illinois at Urbana-Champaign, Urbana IL 61801

Patrick Moriarty[6]
National Renewable Energy Laboratory, Golden, CO, 80401

To alleviate the mass-scaling issues associated with conventional upwind rotor blades of extreme-scale wind turbines (≥ 10MW), the inviscid aerodynamics of a load-aligned blade is compared to that of a conventional blade. This fluid-structure load-alignment reduces cantilever loading and has been projected to reduce blade mass by 50% for both morphing and pre-aligned configurations. This alignment also facilitates blade segmentation, so that the combined effect may lead to a 25% reduction in cost of energy. However, previous quantitative analysis has only included structural simulations. Herein, the aerodynamic performance of this concept is investigated with computational fluid dynamics (CFD). This numerical method was first validated two-dimensionally with the S809 airfoil and three-dimensionally with the Unsteady Aerodynamic Experiment (UAE). The results indicated that this inviscid method is reasonable for predicting torque and thrust when the flow is attached, i.e., with moderate angles of attack. This technique was then applied to a 10 MW wind turbine at rated wind speed for both conventional and load-aligned configurations . The aerodynamic load predictions for thrust and torque compared well with the empirically prescribed force distributions, further supporting the morphing and pre-alignment concepts. Extreme flow conditions as well as fully-coupled fluid-structure simulations are recommended to provide improved fidelity and quantification, as well as a more detailed understanding of the load relief and expected mass savings for these concepts.

Nomenclature

α	=	angle of attack
β	=	load-path angle
c	=	airfoil chord length
C	=	centrifugal force
C_l	=	two-dimensional lift coefficient
C_p	=	pressure coefficient
D	=	rotor diameter
F_Q	=	torque force
F_Q'	=	torque force per length

[1] Research Associate, Mechanical and Aerospace Eng., 122 Engineer's Way, and AIAA Member
[2] Research Assistant, Mechanical and Aerospace Eng., 122 Engineer's Way, and AIAA Member
[3] Graduate Research Assistant, Mechanical and Aerospace Eng., 122 Engineer's Way, and AIAA Member
[4] Professor, Mechanical and Aerospace Eng., 122 Engineer's Way, and AIAA Associate Fellow
[5] Associate Professor, Aerospace Eng., 104 S. Wright St., and AIAA Senior Member
[6] Senior Engineer, National Wind Technology Center, and AIAA Associate Fellow

F_Q'* = non-dimensional torque force
G = gravitational force
φ = azimuthal blade angle (ϕ = 0 represents straight up)
r = radial distance from hub
R = radius
σ = peak Von Mises stress
T = thrust force
T' = thrust force per length
T'* = non-dimensional thrust force
V = wind speed
x = horizontal position along airfoil

Subscripts
cut-in = at cut-in wind speed
cut-out = at cut-out wind speed
rated = at rated power conditions
twist = angle of twist along blade

I. Introduction: Extreme-Scale Systems and Load Alignment Concepts

Since 1995, the average wind turbine rated power has increased twenty-fold[1] and economies of scale and higher winds aloft are driving systems to ever larger sizes. As a result, future extreme-scale systems with power levels of 10-20 MW are expected. Such increases will be associated with much larger turbine blades (since power scales approximately with blade radius squared) and thus unfortunately much larger blade masses. For example Crawford[2] estimated that blade weight increases with $R^{2.1}$ as shown in Fig. 1 Other sources[3,4] have proposed even faster scalings of $R^{2.53}$ or even $R^{3.1}$, due to the increasing importance of gravity loads at extreme scales. This blade mass scaling is important since cost is roughly proportional to mass and since the rotor accounts for about 23% of the initial total system cost. Furthermore, many of the other turbine components also increase in cost as the rotor mass increases.[3] Thus, new concepts in turbine blade design are needed to decrease mass for extreme-scale systems.

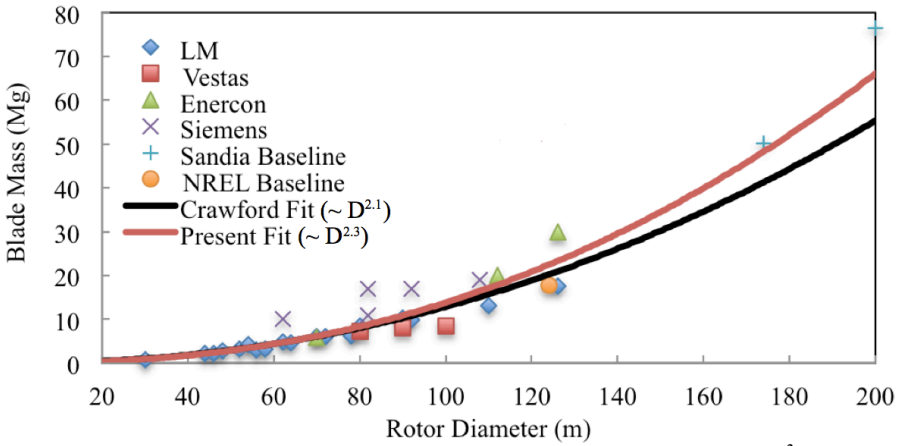

Figure 1. Relationship between blade mass and rotor diameter.[2]

While there have previous attempts to redesign rotor blades based on fluid-structure principles[5], two new concepts have been developed based on load-alignment for extreme-scale systems: segmented ultralight morphing rotors[6] (SUMR) and segmented ultralight pre-aligned rotors[7] (SUPAR). Both concepts use rotor blade downwind orientation that is aligned to minimize loads either for a range of wind speeds by morphing[6], or aligned only at a single optimum wind speed with a fixed geometry[7]. Figure 2 demonstrates the principle of load alignment. Conventional upwind turbine configurations (Fig. 2a) typically employ blades with fiberglass shells (or more expensive but lighter carbon fiber) to carry the structural and aerodynamic loads with very small aeroelastic deflections to avoid tower strikes and fatigue. The resultant of the centrifugal, gravitational, and downwind forces on a conventional blade are shown in Fig. 2b. The combination of these forces leads to cantilever forces in the downwind direction for a conventional blade. Therefore designed stiffness is used to avoid tower strikes and fatigue

leads to the blade mass problems discussed above. This stiffness constraint can be relaxed if a downwind load-aligned concept is employed. A segmented load-aligned blade (Fig. 2c) with a joint at the hub can be unlocked to allow for moment-free downstream morphing or have a pre-set rigid configuration. The alignment angle increases with rated power, meaning downwind cantilever forces (and the associated blade costs) become much more prevalent at extreme-scales.[7]

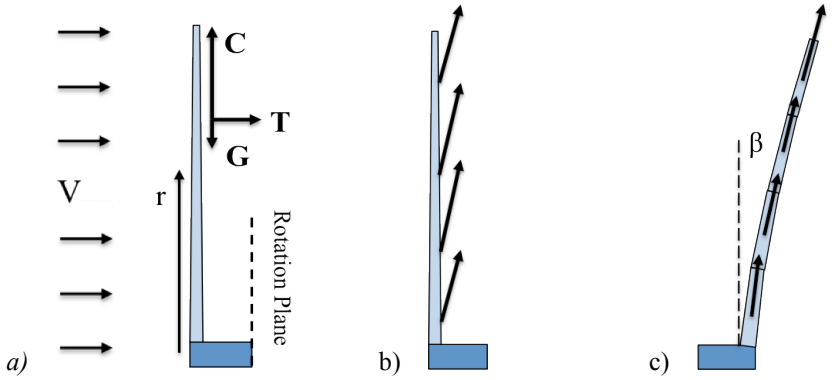

Figure 2. a) Forces on a wind turbine blade viewed perpendicular to the rotor blade, b) the distribution of forces for a conventional upwind rotor blade, and c) the distribution of forces for a load-aligned blade which eliminates cantilever hub moments.

The load-alignment concept is bio-inspired since the low-mass benefits of a morphing design to minimize fluid-structure load in extreme conditions can be observed in nature[6-7]. For example, oak trees have a single section trunk that is stiff and heavy. Under moderate wind conditions, the tree undergoes relatively little deflection, similar to how a conventional turbine blade undergoes little deflection to avoid tower strikes. In high wind conditions, the aerodynamic forces impart extreme cantilever loads on such trees, ultimately destroying them. In contrast, palm trees have a segmented trunk that can easily deflect downwind.[8-10] Under high wind conditions, the flexible living structure can bend downstream and alleviate such destructive cantilever aerodynamic loads. This trunk structure is one of the main reasons that palm trees are much more common near coast lines where hurricane-level winds are common, compared to oak trees and other heavy, stiff trees. Just as the natural flow adaptability of the palm tree handles aerodynamic loads with minimal structural mass, a load-aligned blade (Fig. 2c) can minimize rotor mass by reducing the conventional stiffness constraint. In particular, the blade is aligned so that the structural loads primarily act in tension. The variation in load-path angle over the blade's radius results in the need for a downwind curved blade. To reduce wake effects of the upwind tower on the blade, the tower can be aerodynamically faired. This can have a substantial impact since the drag (and wake of an airfoil) can be many times less than that of a cylinder.

For case of a morphing rotor, the resulting load-path angles (β) will vary as a function of wind speed as shown in Fig. 3. Below the cut-in speed, the blade is held fixed in the conventional orientation. To partially or fully adapt to this change, a hinge between the hub and blade allows for a variable downwind alignment angle for different wind speeds. Below rated conditions, the forces are not large enough to necessitate a full (moment free) morphing angle, so from $V_{cut\text{-}in}$ to V_{rated} the blade linearly morphs from no alignment to the rated condition alignment, and stays aligned up to the cut-out velocity. Past $V_{cut\text{-}out}$ the rotor goes into a parked position. The morphing schedule can also be seen in the following animation, http://www.youtube.com/watch?v=RQmA7JwBefY. Note that the SUPAR concept uses a single geometry, and structural simulations[7] indicated that the blade should be aligned at a wind speed of $1.25V_{rated}$, in order to minimize loads over the entire operating wind speed range. Therefore, the SUMR and SUPAR concepts will both be load-aligned and have the same geometry at $1.25V_{rated}$.

Previous quantitative analysis for SUMR[6] and SUPAR[7] has included finite element analysis for the structural stresses simulations based on empirically estimated aerodynamic loads scaled up from a 5 MW rotor. These studies demonstrated that this load reduction associated with morphing or pre-alignment may reduce cost of energy by as much as 25%. However, no aerodynamic simulations have been conducted to verify that the load-aligned blade can provide similar aerodynamic performance as that of a conventional blade. Herein, the blade aerodynamics are investigated for conventional vs. load-aligned configurations using computational fluid dynamics to examine this important issue.

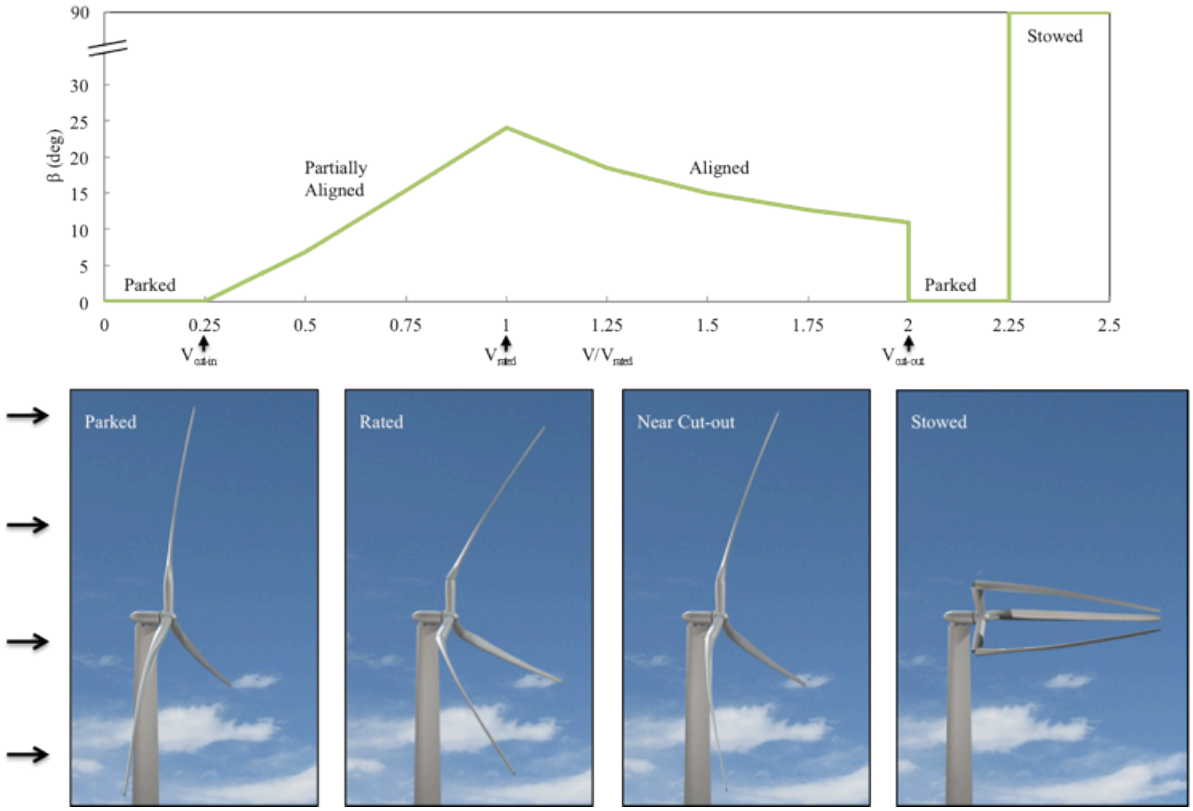

Figure 3. Morphing angle of the SUMR blade vs. wind speed and morphing schedule images.

II. Validation of Aerodynamic Methods

A. S809 Validation

To predict the basic aerodynamic flow features of a wind turbine, ANSYS Fluent (a commercial computational fluid dynamics software package) was used. An inviscid two-dimensional investigation was conducted with the S809 airfoil to determine the fidelity of the code in predicting the wind turbine blade lift aerodynamics. An unstructured mesh was used with a baseline resolution of 100-200 grid points around the airfoil surface. This was compared to a refined mesh with double the number of grid points around the airfoil. The results are shown in Fig. 4 and indicate that this method is reasonable for the linear portion of the lift curve. As expected, the maximum lift and stall performance are not predicted accurately. The reduced computational power for the present formulation, as compared to that for a Reynolds-Averaged Navier-Stokes, is seen as a reasonable trade-off for the lack of performance in predicting viscous effects (such as blade drag and stall effects), which are expected to be minor so long as only steady-state air flow and optimally pitched geometry conditions are considered (as is the case herein).

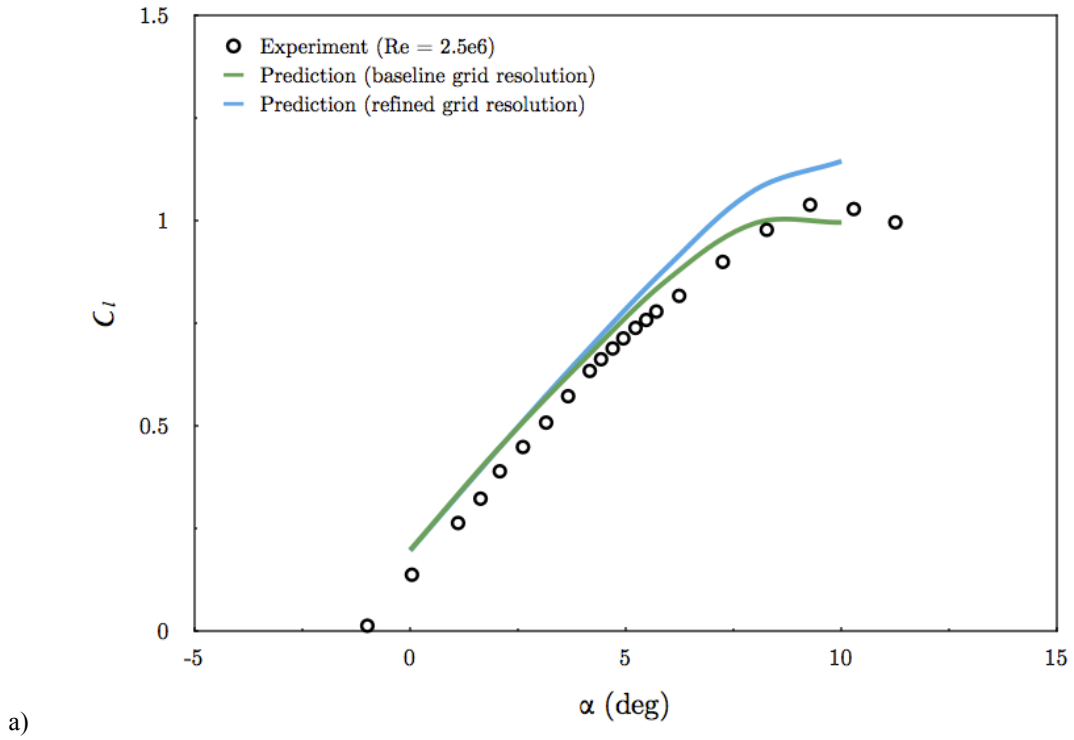

a)

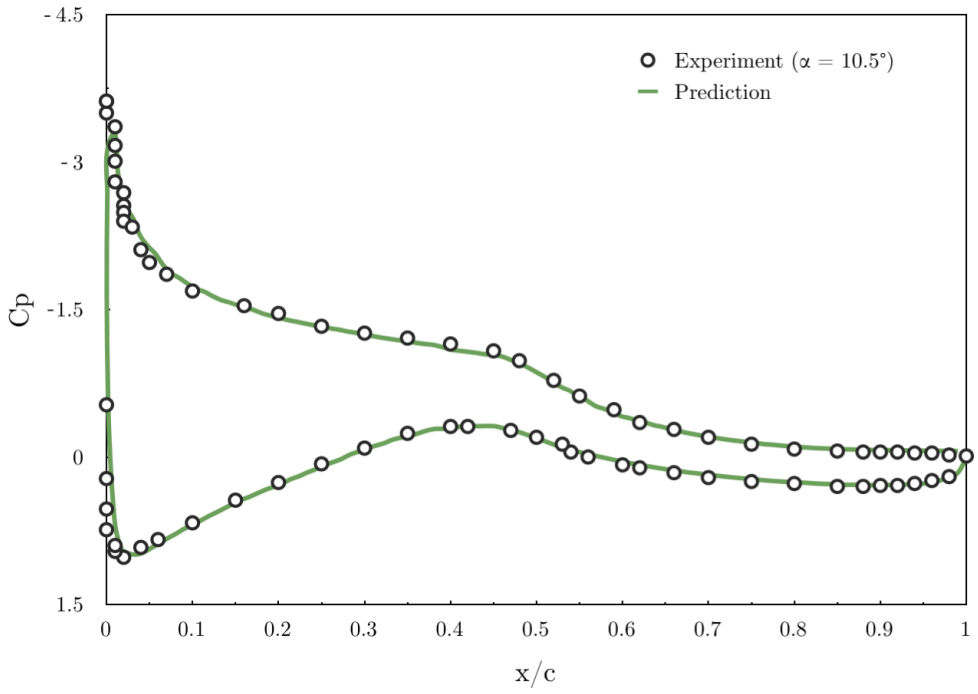

b)

Figure 4. 2-D S809 airfoil comparing experimental results to predictions for lift coefficient for various grid resolutions and b) pressure distribution.

B. UAE Validation

The computational approach was next evaluated using the well-known Unsteady Aerodynamics Experiment (UAE) conducted in the 80'x120' NASA Ames wind tunnel. This rotor is approximately 35' feet in diameter which

utilizes an S809 airfoil cross-section. For the UAE, this airfoil has a chord length and twist distribution along the local radius (r) with a continuous reduction up to the blade radius (R) as shown in Fig. 5.

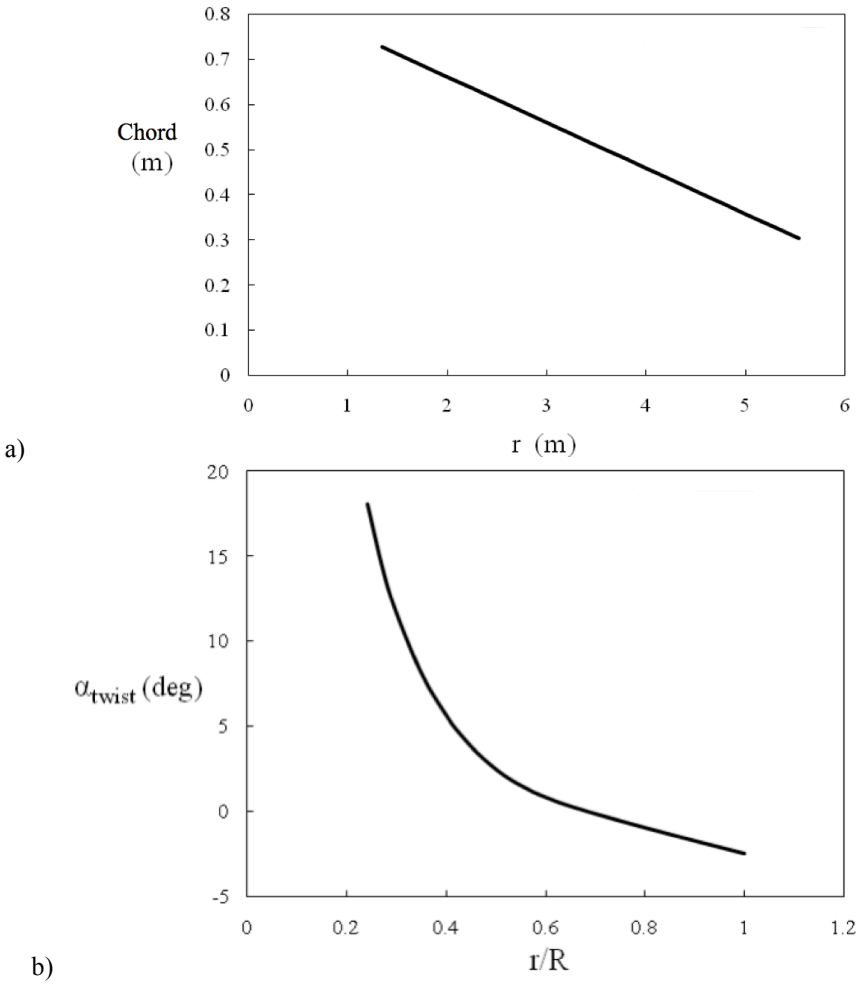

Figure 5. a) Chord and b) twist distribution for the UAE rotor and UAE wind turbine in the NASA Ames 80'x120 wind tunnel

To simply the computational analysis, the computational domain was fixed as a circular cylinder with the same cross-sectional area and streamwise length as the NASA Ames wind tunnel. To reduce computation time, the cylindrical domain was split and a periodic boundary condition was applied for rotational symmetry as shown in Fig 6a. Blade rotation was simulated by adding rotational motion to the reference frame, creating a stationary blade in a swirling flow field. An unstructured mesh was used with 100-200 grid points around the blade surface at any given cross section (Fig 6b). This range was shown to be suitable since higher grid resolutions resulted in little change to the lift curve at moderate angles of attack in the linear portion of the curve (Fig. 4a).

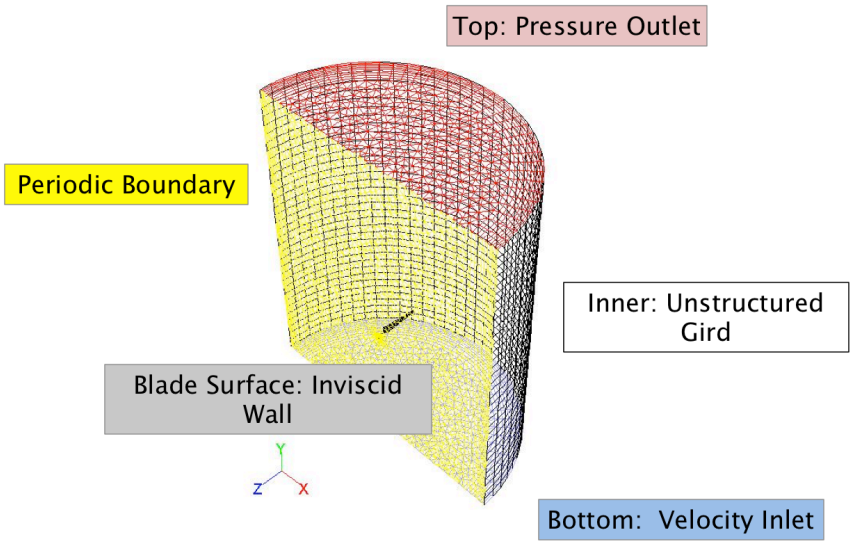

a)

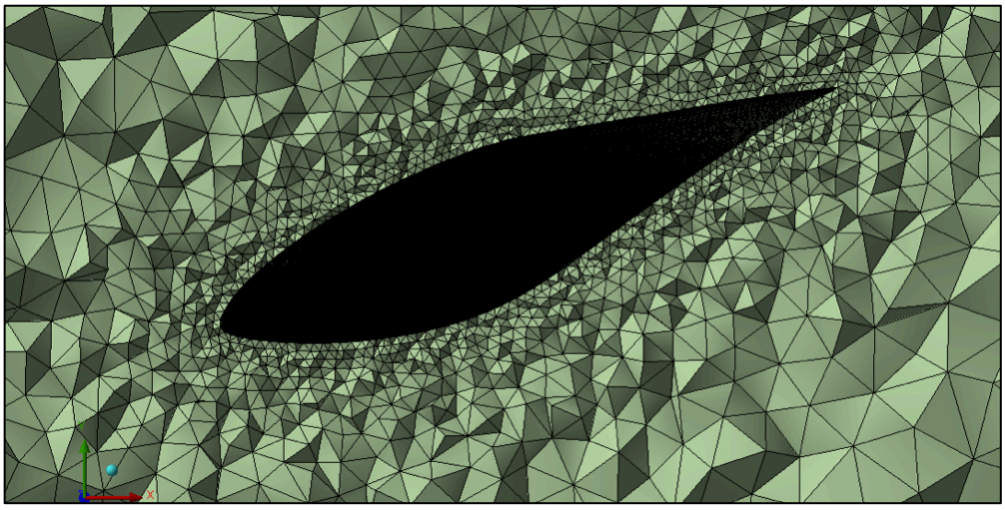

b)

Figure 6. UAE rotor: a) computational domain, b) mesh cross section showing unstructured grid resolution

Sample predicted aerodynamic loads are shown in Fig. 7, where it can be seen that the largest pressure variations (and thus largest aerodynamic loads) are located in the outboard region where the relative velocity is highest. The aerodynamic shaft torque at zero yaw and 3° pitch relative to the tip is shown in Figure 8, and it can be seen that the agreement is reasonable, especially at the lower wind speeds where the tip-speed ratio is highest and closes to typical operating conditions of a wind turbine (at higher wind speeds, flow separation may occur rendering the present inviscid approach less useful and appropriate). In general, the predictions are reasonable for moderate angles of attack so long as the flow is attached, consistent with the variations shown in Fig. 4. These levels of comparison are also similar to predictions reported for several different CFD codes[11] and thus the current method is deemed reasonable for near-rated conditions.

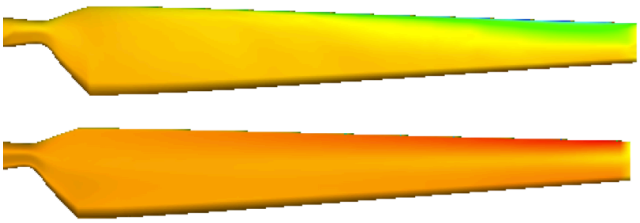

Figure 7. Pressure-side and suction-side pressure distributions at 10 m/s wind speed

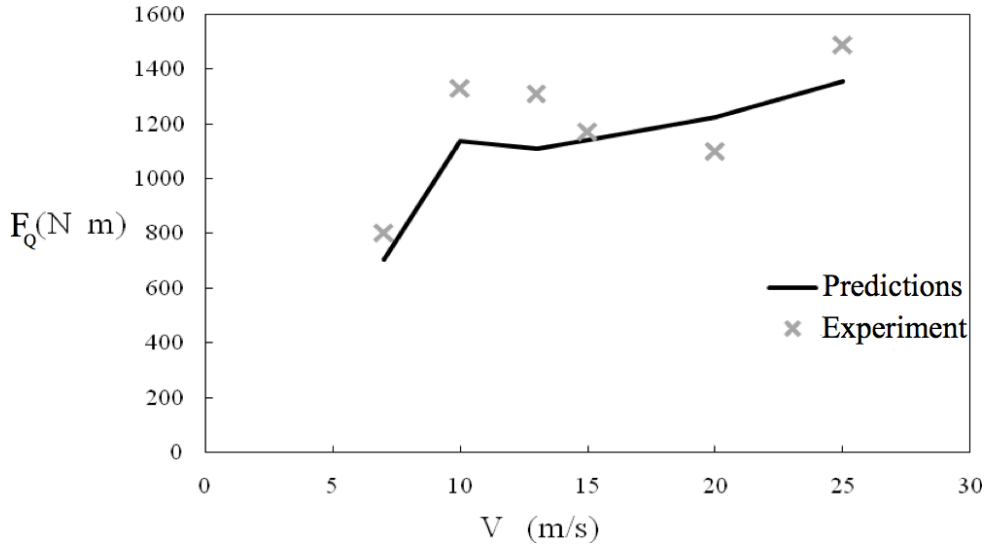

Figure 8. Torque predictions compared to NREL measurements for the UAE in NASA Ames wind tunnel at 3° pitch relative to the tip.

III. Aerodynamics of Conventional vs. Load-Aligned Extreme-Scale Blades

A. Conventional 10 MW Rotor Blade Geometry

The blade geometry for a 10 MW conventional and load-aligned rotor blade is based on the National Renewable Energy Laboratory (NREL) offshore 5 MW baseline wind turbine.[12] This data was then scaled to a 10 MW design with a radius of 82 m.[13] The scaled data used for the model is summarized in Table 1. The NREL 5 MW turbine specifies the airfoils at specific nodes along the blade, as are shown in the right column of Table 1. The hub of the blade is modeled as a cylinder, which at 15% of the blade radius transitions into a 40%-thick, Delft University DU40 airfoil. The 40% thickness airfoil then transitions to a thinner airfoil and at three-quarters of the blade radius becomes a NACA 64, 18%-thick, airfoil. The blade remains a NACA 64 airfoil until the tip. The chord distribution was obtained by using the same non-dimensional chord distribution as that of the NREL 5 MW that has a maximum chord length at approximately 25% of the blade radius.[12] The airfoil distribution, airfoil thickness, and blade twist are shown in Fig. 9.

Table 1. Blade geometry for a scaled 10 MW off-shore wind turbine

Node	Radius [m]	Chord Length [m]	Blade Twist [deg]	Airfoil
1	3.81	4.61	13.31	Cylinder
2	7.45	5.02	13.31	Cylinder
3	11.09	5.42	13.31	Cylinder
4	15.63	5.93	13.31	DU40
5	21.09	6.05	11.48	DU35
6	26.54	5.80	10.16	DU35
7	32.00	5.53	9.01	DU30
8	37.45	5.22	7.80	DU25
9	42.91	4.88	6.54	DU25
10	48.36	4.56	5.36	DU21
11	53.82	4.24	4.19	DU21
12	59.27	3.92	3.13	NACA64
13	64.73	3.60	2.32	NACA64
14	70.18	3.28	1.53	NACA64
15	74.73	3.01	0.86	NACA64
16	78.36	2.72	0.37	NACA64
17	82.00	1.85	0.11	NACA64

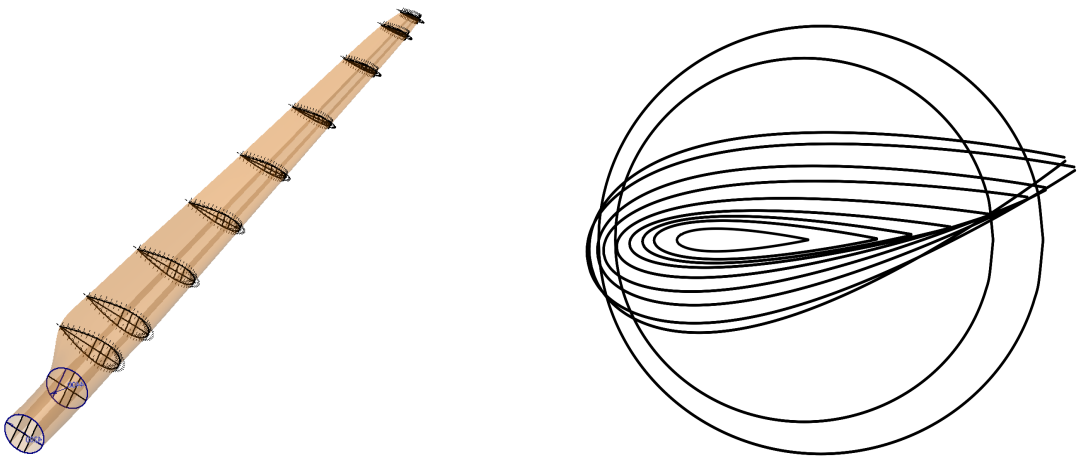

a) b)

Figure 9. a) Airfoil distribution along the blade length showing 11 discrete radial stations, and b) airfoil geometry and blade twist at these same stations.

Similar to the UAE validation, an unstructured mesh was used for the extreme-scale blades with 100-200 grid points around the blade surface at any given cross section. The mesh then became increasingly coarse farther from the surface, producing 550K total grid points within the computational domain for the conventional wind turbine blade (Fig. 10a). For the load-aligned blade, downwind angles for 1.25 V_{rated} were chosen since this condition is consistent with both SUMR and SUPAR concepts, as discussed in Section I. The geometry and mesh for this blade are shown in Fig. 10b.

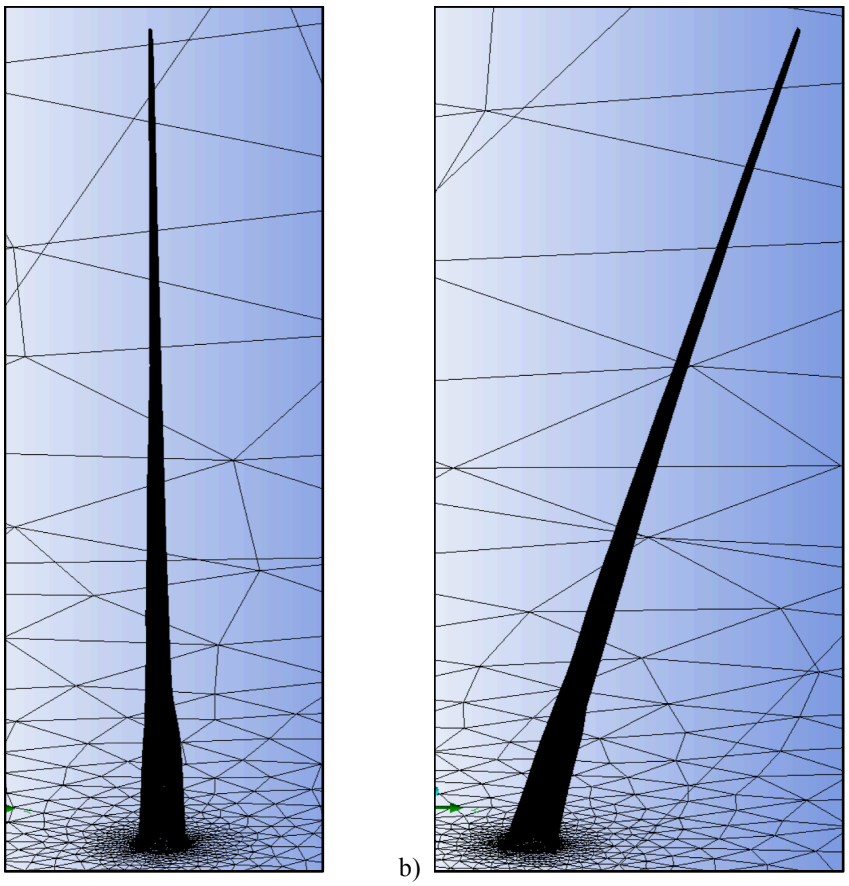

Figure 10. Unstructured mesh for blade surface and periodic boundary for a) conventional blade and b) load-aligned blade, providing a visual representation of the downwind load-alignment angle used in the simulations.

Based on the CFD solutions for these two configurations of Fig. 10, pressure distributions were obtained over the blade surfaces. As shown in Fig. 11, the largest pressure variations for both blades are located in the outboard region where the relative velocity is highest, similar to the UAE condition (Fig. 7). When comparing the conventional blade with the load-aligned blade, the pressure distributions are very similar. This result suggests that the aerodynamic loads are also similar. However, it can be seen that the load-aligned blade has a slight shift of aerodynamic loading away from the outboard sections. The velocity distributions just above the blade surfaces were also examined at the 80% outboard station (r/R=0.8), where the conventional and load-aligned case gave nearly identical distributions suggesting no adverse aerodynamic effects associated with the coned and curved blade.

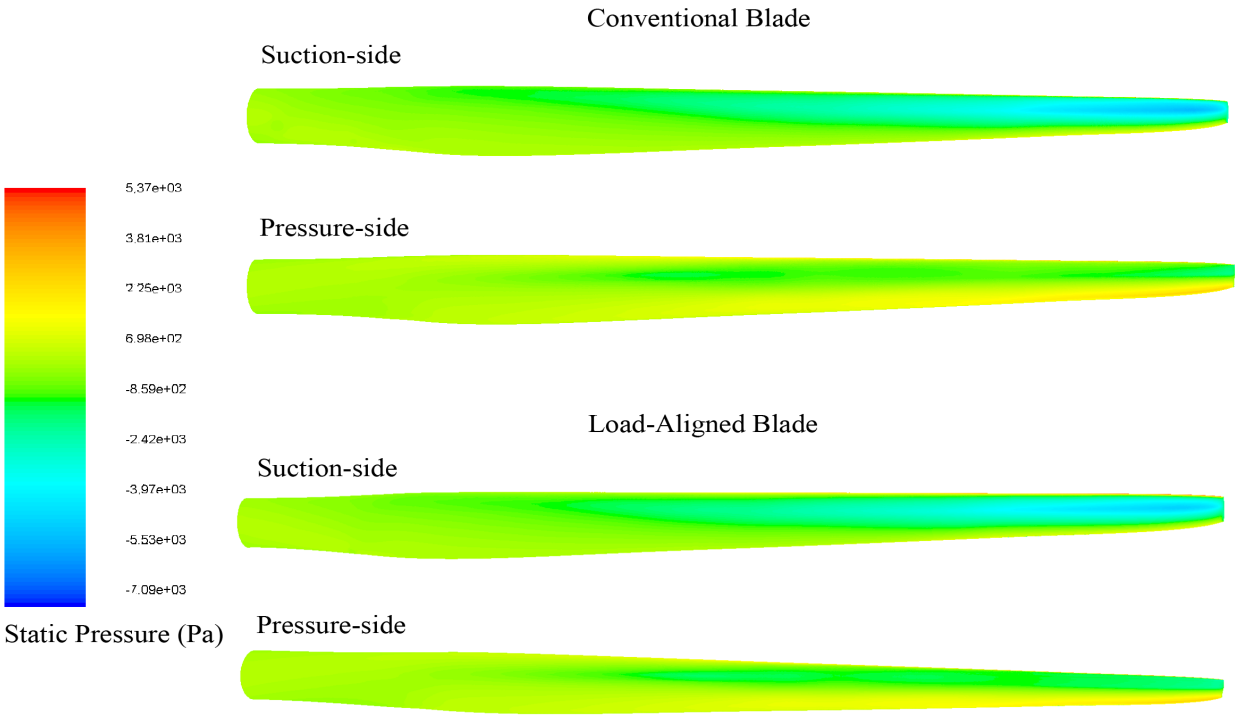

Figure 11. Pressure-side and suction-side pressure distributions for conventional and load-aligned rotor blade at rated power.

To quantify the load distribution differences between the blades and between the empirical distributions used previously[6-7], the thrust and torque force per unit span-length of blade (T' and F_Q') were made non-dimensional based on equation 1 and 2 to compare the approaches.

$$F_Q{}'^* = F_Q{}'\left(\frac{R^2\omega}{P}\right) \tag{1}$$

$$T'^* = T'\left(\frac{R^2\omega}{P}\right) \tag{2}$$

As shown in Fig. 12, the previous empirical distributions match the CFD predictions reasonably well for the radial distribution of both the thrust and torque force on a conventional blade. However, the CFD results tend to show a more even load distribution, while the empirical approximation slightly over-predicts the forces in the intermediate sections ($0.4<r/R<0.9$). It can also be seen that the CFD predictions of torque for the load-aligned blade forces are very similar to the conventional blade, where the same disk area has been maintained by use of a longer blade for the load-aligned case. However, the load-aligned blade tends to show slightly higher thrust values indicating that there is a non-linear pitch coupling due to the coning which affects the angle of attack. This indicates that a conventional pitch schedule would need to be modified somewhat for a load-aligned blade. The most important conclusion of these simulations is that load-alignment does not have an adverse aerodynamic effect on the thrust and torque forces produced. This supports the mass and cost savings previously projected from structural simulations[6-7].

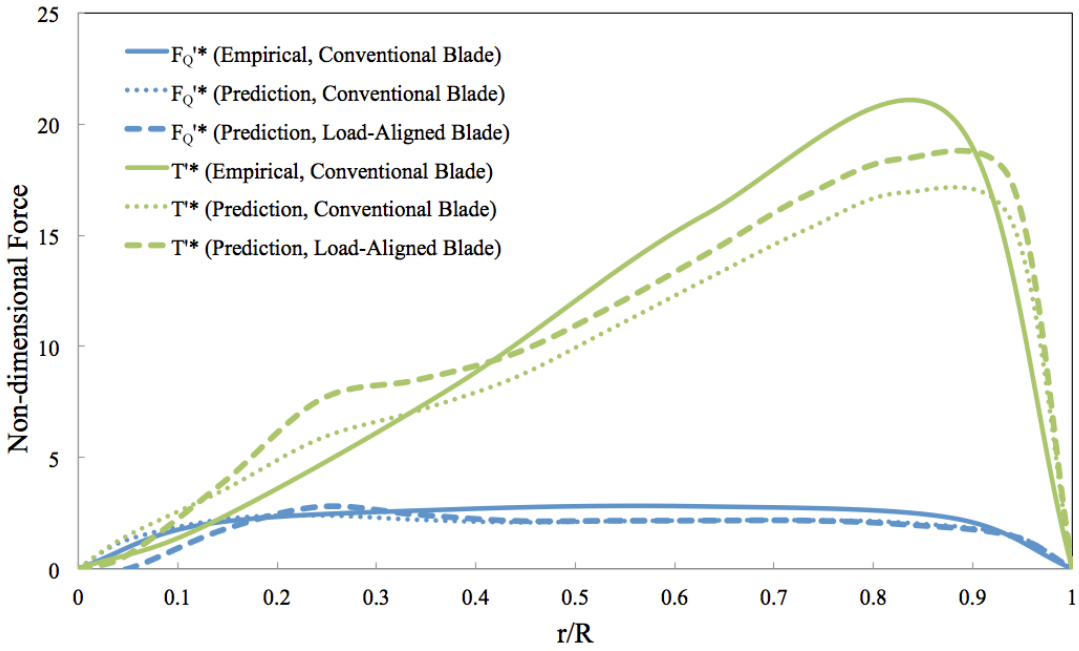

Figure 12. Radial distribution of non-dimensionalized torque force and thrust comparing previous first order approximations to the current CFD simulations for a conventional blade, as well as comparing conventional and load-aligned blade force distributions.

IV. Conclusions and Recommendations

To alleviate the mass-scaling issues associated with conventional upwind rotors of extreme-scale wind turbines (≥ 10MW), a load-aligned blade was investigated in conjunction with recent proposals for two new concepts: a segmented ultralight morphing rotor (SUMR) and a segmented ultralight pre-aligned rotor (SUPAR). The load-aligned concept employs a downwind rotor with coned and curved blades to allow for moment-free downstream alignment. This alignment leads to primarily tensile loading (rather than cantilever) along the blade direction and may provide a net mass savings of 50%. This study is the first to investigate the aerodynamic performance of the load-aligned concept. An inviscid computational fluid dynamics (CFD) method was validated two-dimensionally with the S809 airfoil and three-dimensionally with the UAE conducted in the 80x120 ft NASA Ames wind tunnel. The CFD results indicated that this method is reasonable for predicting torque and thrust at moderate angles of attack when the flow is attached, consistent with steady-state operation near rated conditions. Application of this same method to a load-aligned blades for a 10 MW turbine at a wind speed equal to 1.25 times rated wind speed (where the SUMR and SUPAR geometries are consistent) yielded very similar velocity pressure distributions when compared to a conventional blade at the same conditions (though the load-aligned blade has a slight shift of aerodynamic loading away from the outboard sections). Examination of the detailed thrust and torque distributions as a function of radius also showed that the conventional and load-aligned case gave nearly identical distributions suggesting no adverse aerodynamic effects associated with the coned and curved blade. Furthermore, previous empirical aerodynamic load distributions (used to demonstrate the SUMR and SUPAR concepts) were found to reasonably match the CFD predictions (though the CFD results tend to show a more even load distribution). This general agreement supports the mass and cost savings previously projected from structural simulations, but suggest that fully-coupled fluid-structure simulations be completed to further quantity and assess the load-alignment concept. In addition, investigations for a range of wind speeds, including extreme winds associated with stowed conditions are needed to determine the robustness of these concepts. Such simulations can pave the way to experimental and design studies which are critical to determine the viability of the SUMR and SUPAR concepts.

References

[1]Ashwill, T.D., "Materials and Innovations for Large Blade Structures: Research Opportunities in Wind Energy Technology," *AIAA/ASME/ASCE/AHS, ASC Structures, Structural Dynamics, and Materials Conference*, AIAA 2009-2407, 2009.

[2]Crawford, C., "The Path from Functional to Detailed Design of a Coning Rotor Wind Turbine Concept", *CDEN/C2E2 Conference*, Winnipeg, Manitoba, July 22–24, 2007

[3]Rasmussen, F., Petersen, J.T., Volund, P. Leconte, P, Szechenyi, E and Westergaard, C. "Soft Rotor Design for Flexible Turbines", Riso National Laboratory, Roskilde, Denmark, Contract JOU3-CT95-0062.

[4]Griffith, T. and Ashwill, T., "The Sandia 100-meter All-glass Baseline Wind Turbine Blade: SNL100-00", Albuquerque, NM: Sandia National Laboratories, SAND2011-3779, 2011.

[5]Rasmussen, F., Petersen, J.T., Volund, P. Leconte, P, Szechenyi, E and Westergaard, C. "Soft Rotor Design for Flexible Turbines", Roskilde, Denmark: Riso National Laboratory, Contract JOU3-CT95-0062.

[6]Ichter, B., Steele, A., Loth, E., and Moriarty, P., "Structural Design and Analysis of a Segmented Ultralight Morphing Rotor (SUMR) for Extreme-Scale Wind Turbines", *42nd AIAA Fluid Dynamics Conference and Exhibit*, New Orleans, LA, AIAA-2012-3270, June 2012.

[7]Loth, E., Steele, A., Ichter, B., Selig, M., and Moriarty, P., "Segmented Ultralight Pre-Aligned Rotor for Extreme-Scale Wind Turbines", *AIAA Aerospace Sciences Meeting*, Nashville, TN, AIAA-2012-1290, January 2012.

[8]NOAA, "Pam Tree Bending" [online], www.photolib.noaa.gov/ [retrieved June 2011].

[9]Brooks, J., "Hurricane Dennis batters palm trees and floods parts of Naval Air Station (NAS) Key West's Truman Annex" [online], www.navy.mil/ [retrieved May 2012].

[10]Isanagorski, "Hurricane_2" [online], palmbeachcountyextension.wordpress.com/ [retrieved May 2012].

[11]Simms, D., Schreck, S., Hand, M., Fingersh, L. J. (2001). NREL Unsteady Aerodynamics Experiment in the NASA-Ames Wind Tunnel: A Comparison of Predictions to Measurements. 52 pp.; NREL Report No. TP-500-29494.

[12]Jonkman, J., Butterfield, S., Musial, W., and Scott, G., *Definition of a 5-MW Reference Wind Turbine for Offshore System Development*, Golden, CO: NREL Technical Publishing, NREL/TR-500-38060, February 2009.

[13]Hillmer, B, T. Borstelmann, A.P. Schaffarczyk and L. Dannenberg, *Aerodynamic and Structural Design of MultiMW Wind Turbines beyond 5 MW*, Journal of Physics, Conf. Series, 75, 012002, 2007.

[14]Hartwanger, D., and Horvat, A., "3D Modeling of a Wind Turbine Using CFD", *NAFEMS Conference*, United Kingdom, 2008.